LETTER

doi:10.1038/nature11114

The deubiquitinase USP9X suppresses pancreatic ductal adenocarcinoma

Pedro A. Pérez-Mancera[1], Alistair G. Rust[2], Louise van der Weyden[2], Glen Kristiansen[3], Allen Li[4], Aaron L. Sarver[5], Kevin A. T. Silverstein[5], Robert Grützmann[6], Daniela Aust[7], Petra Rümmele[8], Thomas Knösel[9,10], Colin Herd[11], Derek L. Stemple[11], Ross Kettleborough[11], Jacqueline A. Brosnan[4], Ang Li[4], Richard Morgan[4], Spencer Knight[4], Jun Yu[4], Shane Stegeman[12], Lara S. Collier[13], Jelle J. ten Hoeve[14,15], Jeroen de Ridder[14], Alison P. Klein[4], Michael Goggins[4], Ralph H. Hruban[4], David K. Chang[16,17,18], Andrew V. Biankin[16,17,18], Sean M. Grimmond[19], Australian Pancreatic Cancer Genome Initiative†, Lodewyk F. A. Wessels[14,15], Stephen A. Wood[12], Christine A. Iacobuzio-Donahue[4]*, Christian Pilarsky[6]*, David A. Largaespada[20]*, David J. Adams[2] & David A. Tuveson[1]

Pancreatic ductal adenocarcinoma (PDA) remains a lethal malignancy despite much progress concerning its molecular characterization. PDA tumours harbour four signature somatic mutations[1–4] in addition to numerous lower frequency genetic events of uncertain significance[5]. Here we use *Sleeping Beauty* (SB) transposon-mediated insertional mutagenesis[6,7] in a mouse model of pancreatic ductal preneoplasia[8] to identify genes that cooperate with oncogenic *Kras*^{G12D} to accelerate tumorigenesis and promote progression. Our screen revealed new candidate genes for PDA and confirmed the importance of many genes and pathways previously implicated in human PDA. The most commonly mutated gene was the X-linked deubiquitinase *Usp9x*, which was inactivated in over 50% of the tumours. Although previous work had attributed a pro-survival role to *USP9X* in human neoplasia[9], we found instead that loss of *Usp9x* enhances transformation and protects pancreatic cancer cells from anoikis. Clinically, low USP9X protein and messenger RNA expression in PDA correlates with poor survival after surgery, and USP9X levels are inversely associated with metastatic burden in advanced disease. Furthermore, chromatin modulation with trichostatin A or 5-aza-2′-deoxycytidine elevates *USP9X* expression in human PDA cell lines, indicating a clinical approach for certain patients. The conditional deletion of *Usp9x* cooperated with *Kras*^{G12D} to accelerate pancreatic tumorigenesis in mice, validating their genetic interaction. We propose that *USP9X* is a major tumour suppressor gene with prognostic and therapeutic relevance in PDA.

The biological sequelae of PDA has been partially attributed to frequent and well characterized mutations in *KRAS* (>90%), *CDKN2A* (>90%), *TP53* (70%) and *SMAD4* (55%)[1–4]. Recent genome-wide analyses have uncovered numerous additional somatic genetic alterations, although the functional relevance of most remains uncertain[5]. To explore the molecular genesis of PDA we previously generated a mouse model of pancreatic intraepithelial neoplasia (mPanIN) by conditionally expressing an endogenous *Kras*^{G12D} allele in the developing pancreas[8]. Mice with mPanIN spontaneously progress to mouse PDA (mPDA) after a long and variable latency, providing an opportunity to characterize genes that cooperate with *Kras*^{G12D} to promote early mPDA. We hypothesized that such genes could be directly identified by applying insertional mutagenesis strategies[6,7,10,11] in our mPanIN model, and that these candidates could represent 'drivers' of PDA development.

Accordingly, we interbred our mPanIN model with two distinct SB transposon systems and monitored mice for early disease progression. Our initial approach used the well characterized *CAGGS-SB10* transgenic allele to promote transposition[6]. Although *CAGGS-SB10* promoted PDA, a variety of non-pancreatic neoplasms and a paucity of identified common insertion sites (CIS) in the recovered pancreatic neoplasms precluded a comprehensive analysis, potentially reflecting the variegated expression of *CAGGS-SB10* (ref. 12) (Supplementary Figs 1a and 2, and Supplementary Tables 1 and 3b).

To increase the specificity and potency of SB mutagenesis, we generated a conditional *SB13* mutant mouse by targeting the *Rosa26* locus in embryonic stem cells (Supplementary Fig. 3a, b). The pancreas-specific expression and function of the conditional *SB13* allele was confirmed (Supplementary Fig. 3c), and we found that SB13-induced transposition by itself did not promote lethality or pancreatic tumorigenesis (Fig. 1a and Supplementary Fig. 4a). In contrast, *Kras*$^{LSL\text{-}G12D}$; *Pdx1-cre; T2/Onc; Rosa26-LSL-SB13* mice rapidly progressed and succumbed to invasive pancreatic neoplasms (Fig. 1a–c). A cohort of 117 *Kras*$^{LSL\text{-}G12D}$; *Pdx1-cre; T2/Onc; Rosa26-LSL-SB13* mice (Supplementary Fig. 1b) was monitored for tumour development, and 103 of these mice were available for full necropsy and tissue procurement. The majority of such mice harboured multi-focal pancreatic tumours, and 198 distinct primary tumours and metastases were subjected to histological and molecular analysis. Most mice had invasive carcinomas (66 of 103) that consisted of classical mPDA (78.8%) or invasive cystic neoplasms (21.2%); 34.8% of mice also contained metastases predominantly in their liver and lungs (Supplementary Fig. 4c). The remainder of the mice (37 of 103) had pre-invasive pancreatic tumours consisting of high-grade

[1]Li Ka Shing Centre, Cambridge Research Institute, Cancer Research UK, and Department of Oncology, Robinson Way, Cambridge CB2 0RE, UK. [2]Experimental Cancer Genetics, Wellcome Trust Sanger Institute, Hinxton CB10 1SA, UK. [3]Institute of Pathology, University Hospital of Bonn, Sigmund-Freud-Str. 25, 53127 Bonn, Germany. [4]Departments of Oncology and Pathology, The Sol Goldman Pancreatic Cancer Research Center, Johns Hopkins Medical Institutions, Baltimore, Maryland 21231, USA. [5]Biostatistics and Bioinformatics Core, Masonic Cancer Center, University of Minnesota, 425 Delaware St SE MMC 806, Minneapolis, Minnesota 55455, USA. [6]Department of Surgery, University Hospital Dresden, Fetscherstr. 74, 01307 Dresden, Germany. [7]Institute of Pathology, University Hospital Dresden, Fetscherstr. 74, 01307 Dresden, Germany. [8]Institute of Pathology, University of Regensburg, Franz-Josef-Strauss-Allee 11, 93053 Regensburg, Germany. [9]Institute of Pathology, University Hospital of Jena, Bachstraße 18, 07743 Jena, Germany. [10]Institute of Pathology, Ludwig-Maximilians-University (LMU), Thalkirchnerstr. 36, 80337 Munich, Germany. [11]Vertebrate Development and Genetics, Wellcome Trust Sanger Institute, Hinxton CB10 1SA, UK. [12]Eskitis Institute for Cell and Molecular Therapies, Griffith University, Nathan, Queensland 4111, Australia. [13]School of Pharmacy, University of Wisconsin, Madison, Wisconsin 53705, USA. [14]Delft Bioinformatics Lab, Faculty of EEMCS, Delft University of Technology, 2628 CD Delft, The Netherlands. [15]Bioinformatics and Statistics, The Netherlands Cancer Institute, Plesmanlaan 121, 1066 CX Amsterdam, The Netherlands. [16]The Kinghorn Cancer Centre, Cancer Research Program, Garvan Institute of Medical Research, 372 Victoria St, Darlinghurst, Sydney, New South Wales 2010, Australia. [17]Department of Surgery, Bankstown Hospital, Eldridge Road, Bankstown, Sydney, New South Wales 2200, Australia. [18]South Western Sydney Clinical School, Faculty of Medicine, University of NSW, Liverpool, New South Wales 2170, Australia. [19]Queensland Centre for Medical Genomics, Institute for Molecular Bioscience, University of Queensland, St Lucia, Brisbane, Queensland 4072, Australia. [20]Masonic Cancer Center, University of Minnesota, Minneapolis, Minnesota 55455, USA.

*These authors contributed equally to this work.

†Lists of participants and their affiliations appear at the end of the paper.

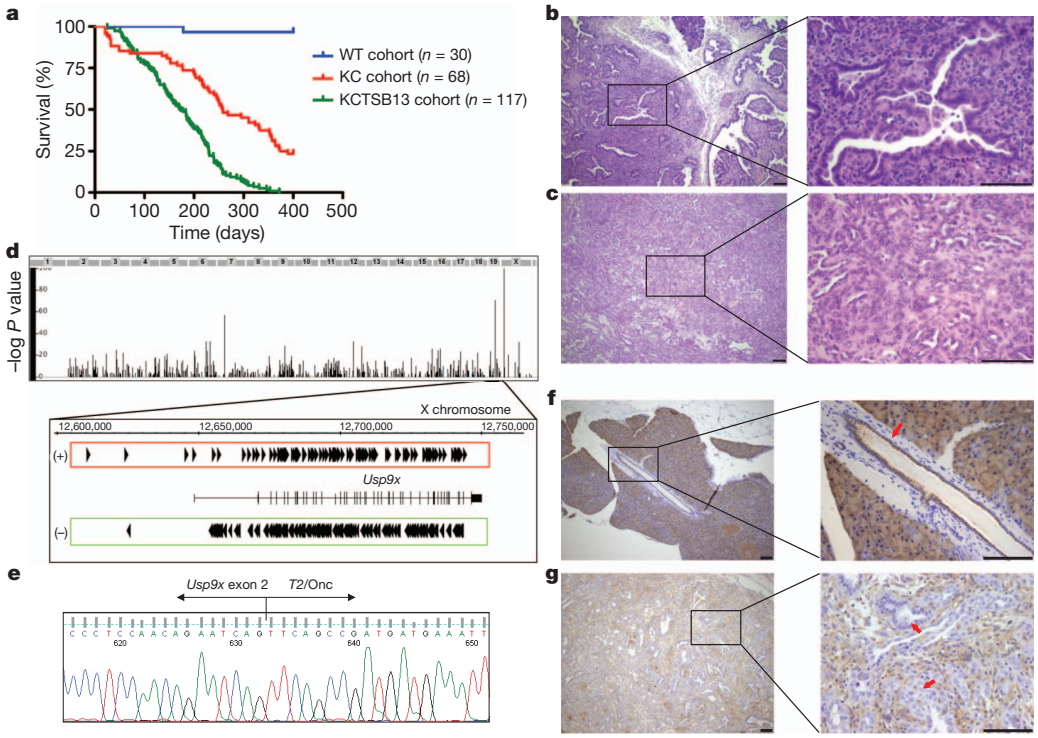

Figure 1 | Transposon mutagenesis accelerates murine PDA and targets Usp9x. **a**, Increased mortality of *Kras*$^{LSL\text{-}G12D}$; *Pdx1-cre; T2/Onc; Rosa26-LSL-SB13* (KCTSB13) mice compared to the KC cohort (containing *Kras*$^{LSL\text{-}G12D}$; *Pdx1-cre; T2/Onc*, *Kras*$^{LSL\text{-}G12D}$; *Pdx1-cre*; *Rosa26-LSL-SB13* and *Kras*$^{LSL\text{-}G12D}$; *Pdx1-cre* mice) (172 versus 257 days, $P < 0.001$; long-rank test). The wild-type (WT) cohort comprises *Kras*$^{LSL\text{-}G12D}$; *T2/Onc; Rosa26-LSL-SB13* and *Pdx1-cre; T2/Onc; Rosa26-LSL-SB13* mice. **b**, **c**, Invasive cystic neoplasm (**b**) and mPDA (**c**) in *Kras*$^{LSL\text{-}G12D}$; *Pdx1-cre; T2/Onc; Rosa26-LSL-SB13* mice. Scale bar: 100 μm. **d**, *Usp9x* is the major CIS in *Kras*$^{LSL\text{-}G12D}$; *Pdx1-cre; T2/Onc; Rosa26-LSL-SB13* PDA tumours (*x* axis denotes genome, *y* axis –log *P* value), with bidirectional insertions. (+) indicates parallel to *Usp9x* expression; (−) indicates antiparallel. **e**, *Usp9x* exon 2-*T2/Onc* chimaeric mRNA in SB13 tumours. **f**, **g**, Usp9x protein expression in normal pancreatic ducts (arrow) (**f**), but not in neoplastic cells (arrows) (**g**), in SB13 PDA harbouring Usp9x insertions. Scale bar: 100 μm.

mPanIN and cyst-forming papillary neoplasms (Supplementary Fig. 4b).

The candidate genes identified from the SB13 screen represented unanticipated candidates as well as many genes and pathways previously implicated in human PDA (Table 1 and Supplementary Tables 2, 3a and 4). Indeed, various members of the TGF-β pathway, including *Smad3*, *Smad4*, *Tgfbr1* and *Tgfbr2*, were collectively mutated in 32% of the tumours. Also, the Rb–p16Ink4a pathway was disrupted in 21% of the tumours. CISs representing the orthologues of additional human PDA genes included *Fbxw7* (24.2%), *Arid1a* (19.1%), *Acvr1b* (19.1%), *Stk11* (also called *Lkb1*) (6.5%), *Mll3* (6%), *Smarca4* (6%) and *Pbrm1* (4.5%)[5,13–15]. *Trp53* was the only commonly mutated PDA gene conspicuously absent, although the p53 regulatory deubiquitinase Usp7 was a CIS (6.5%)[16]. Several CISs previously noted in insertional mutagenesis screens for hepatocellular carcinoma or gastrointestinal tract adenomas, but not typically mutated in PDA, were also identified in this study, including *Zbtb20*, *Nfib* and *Ube2h* in liver tumours[10], and *Pten*, *Tcf12*, *Ppp1r12a* and *Ankrd11* in gastrointestinal tract adenoma/adenocarcinoma[11]. This indicates that many tumour progression pathways may be common to pancreatic, liver and gastrointestinal/colorectal tumours.

Table 1 | Top 20 candidate CIS genes that cooperate with *Kras*^{G12D} to promote mPDA in *Kras*$^{LSL\text{-}G12D}$; *Pdx1-cre; T2/Onc; Rosa26-LSL-SB13* mice

Gene	Chr	CIS peak location	CIS height	*n*	*l*	Mutation in humans
Usp9x	X	12691773	158.1266	101	341	–
Pten	19	32872602	64.5204	61	96	–
Fndc3b	3	27562591	13.7096	55	67	–
Setd5	6	113057997	35.6176	52	71	–
Arfip1/Fbxw7	3	84769635	21.6666	48	80	Yes (ref. 5)
Fam193a	5	34705809	24.3555	45	78	–
Ctnna1	18	35342868	20.2017	45	50	–
Magi1	6	93859940	13.3715	43	57	–
Mkln1	6	31414109	16.5263	41	53	–
Pum1	4	130288478	12.7948	41	46	Yes (ref. 5)
Farp1	14	121587858	9.407	39	47	–
Foxp1	6	98921646	19.5831	38	60	–
Arid1a	4	133268936	32.1628	38	47	Yes (ref. 5)
Acvr1b	15	101024934	31.1752	38	47	Yes (ref. 15)
Map4k3	17	81109860	13.2385	38	45	Yes (ref. 5)
Stag2	X	39535994	16.8613	37	48	–
Mll5	5	22982314	16.0001	37	43	Yes (ref. 5)
Atxn2/Sh2b3	5	122267680	12.3174	37	41	–
Arhgap5	12	53644560	37.416	35	61	–
Gsk3b	16	38106972	21.79	35	43	–

CISs were ranked by tumour frequency where the spatial distribution of insertion sites was analysed using the narrowest 15K kernel scale. Chr, chromosome; CIS height, estimate of the number of insertions within a specific genomic region as a result of summing the kernel functions present in that region; *l*, total number of insertions of the CIS in the indicated tumours; *n*, number of tumours from which the CIS was found.

Unexpectedly, the most frequent CIS observed was the X-linked deubiquitinase *Usp9x*, a gene that had not been previously associated with PDA or other types of carcinoma in humans or mouse models. Indeed, the COSMIC data base revealed only one *USP9X* mutation in a case of ovarian cancer, although the functional relevance of this mutation has not been characterized (COSMIC mutation ID 73237). *Usp9x* was disrupted in over 50% of all tumours, with 341 insertions noted in the 101 tumours harbouring this CIS (Fig. 1d and Table 1). Furthermore, *Usp9x* was also identified as a CIS in four samples from the initial SB10 screen (Supplementary Table 1), supporting its candidacy as a PDA genetic determinant. We confirmed that *Usp9x* was disrupted in tumours by isolating chimaeric fusion mRNAs that spliced the *Usp9x* transcript to the *T2/Onc* transposon (Fig. 1e). In addition, the Usp9x protein was specifically absent in neoplastic cells in pancreatic tumours bearing intragenic insertions (Fig. 1f, g).

To characterize the cellular and molecular pathways affected by *Usp9x* in PDA, we used RNA interference to deplete *Usp9x* levels in

mPDA cell lines (Supplementary Fig. 5a). Although *Usp9x* depletion did not affect the proliferation of monolayer cultures (Supplementary Fig. 5b), it significantly increased colony formation in soft agar (Fig. 2a, Supplementary Fig. 5c) compared to cells transfected with scrambled short hairpin RNAs. Furthermore, knock down of *Usp9x* potently suppressed anoikis in mPDA cells (Fig. 2b). These properties of Usp9x were predominantly dependent on its intrinsic deubiquitinase activity (Supplementary Fig. 6a, b).

Because USP9X was previously reported to positively regulate SMAD4 transcriptional activity[17] and *SMAD4* is commonly mutated in PDA[4], we hypothesized that *Usp9x* loss would attenuate Smad4 function or TGF-β responsiveness in PDA cell lines. However, irrespective of Usp9x expression level, mPDA cell lines expressed Smad4 and were equally sensitive to p21 induction, growth inhibition and morphological alterations after exposure to TGF-β1 (Supplementary Fig. 7). Therefore, we were unable to ascribe a specific role to Usp9x in the regulation of the Smad4–TGF-β pathway in mPDA cells or tumours.

We next investigated several additional proteins reported to be regulated by Usp9x and involved in pathways relevant to cellular transformation. Although USP9X has been shown to bind to and regulate two proteins involved in cell survival, ASK1 (ref. 18) and MCL1 (refs 9, 19), we could not detect obvious changes in Ask1 or Mcl1 protein levels upon *Usp9x* loss (Fig. 2c). Usp9x has also been reported to deubiquitinate and thereby stabilize the E3 ligase Itch[20]; decreased protein levels of Itch were observed in mouse and human PDA cells upon the depletion of Usp9x (Fig. 2c and Supplementary Fig. 8a). Notably, ectopic Itch expression was sufficient to promote anoikis in mPDA cells (Fig. 2d), and Itch was partially responsible for the ability of Usp9x to promote anoikis and suppress colony formation (Supplementary Fig. 6c, d). Because Itch is known to promote the degradation of several proteins relevant to cell proliferation and survival[21], we evaluated the protein expression of likely candidates

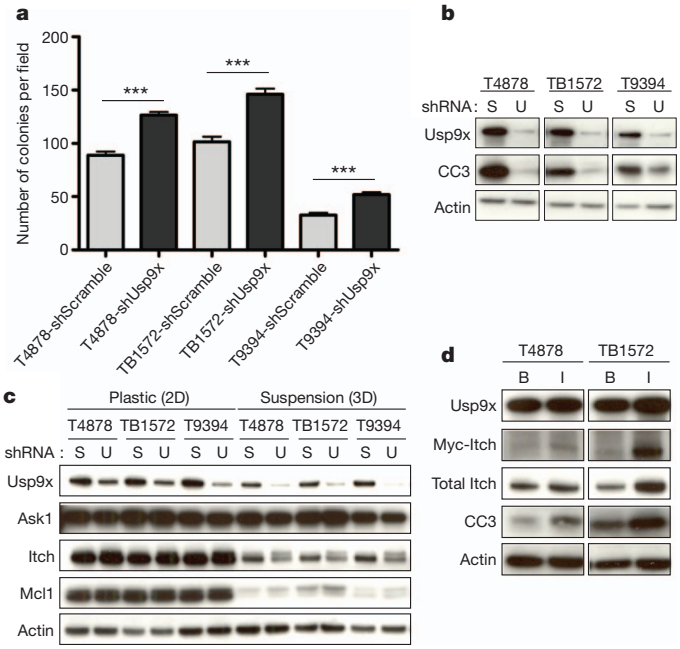

Figure 2 | Usp9x regulates PDA cellular transformation and Itch. **a**, **b**, Usp9x knock down promotes anchorage-independent growth in three mPDA cell lines (**a**), and decreases anoikis denoted by cleaved caspase 3 (CC3) (**b**). The mean and s.e.m. of one representative experiment performed in triplicate are shown in **a** (***$P < 0.001$; Mann–Whitney *U*-test). S, scramble; U, Usp9x. **c**, Usp9x knock down decreases Itch levels but not Ask1 or Mcl1 levels. Changes in Itch are more evident in suspension cultures, and the slower migrating band has the expected mobility of mono-ubiquitinated Itch. **d**, Ectopic Itch induces anoikis. B, pBabe-neo; I, pBabe-neo-Myc-Itch.

including c-Jun, p63 and c-Flip but observed no alterations (Supplementary Fig. 8b). Furthermore, the *Itch* gene was identified as a CIS in 13% of cases (Supplementary Table 2). Therefore, Usp9x mutation may promote tumorigenesis in part by disabling Itch function, and the Usp9x–Itch pathway may work to constrain pancreatic tumorigenesis.

To determine whether *USP9X* expression is aberrant in human PDA, three distinct patient cohorts were assessed. First, we analysed a cohort of 100 Australian patients who underwent surgery for localized PDA and had detailed information available concerning clinicopathological characteristics and outcome (Supplementary Fig. 9 and Supplementary Tables 5 and 6). Tumour DNA from 88 patients in this cohort failed to yield somatic mutations in *USP9X*, consistent with previous reports[5] (data not shown). Notably, the low expression of *USP9X* mRNA correlated with poor survival after surgery ($P = 0.0076$) (Fig. 3a), and multivariate analysis revealed that *USP9X* expression was an independent poor prognostic factor after surgery (Supplementary Table 7). We next analysed autopsy specimens from a separate cohort of 42 American patients to determine that USP9X protein expression inversely correlated with a widespread metastatic pattern ($P = 0.0212$) (Fig. 3b), and bore no relation to SMAD4 expression (Supplementary Table 8). A third collection of PDA specimens obtained from resected German patients ($n = 404$) was used to determine that USP9X and ITCH protein levels were decreased (Supplementary Fig. 10) and expressed in a similar manner (Spearman-Rho correlation = 0.47; $P < 0.01$; Supplementary Table 9a) in tumours compared to normal pancreatic tissue. Furthermore, the proportion of tumours that had undetectable USP9X (13.6%) or ITCH (30.5%) protein correlated with a worse outcome (Supplementary Fig. 11, Supplementary Table 9b, c), particularly regarding USP9X in the subset of high-grade tumours (Fig. 3c and Supplementary Tables 10 and 11). Collectively, these findings implicate the loss of USP9X expression as a relevant event in human pancreatic cancer progression.

We found that USP9X was expressed throughout murine and human tumour development and lost focally in PDAs (Supplementary Figs 12 and 13). Additionally, human PDA cell lines expressed lower levels of USP9X compared to non-PDA cancer cell lines (Supplementary Fig. 14). To investigate additional potential mechanisms of *USP9X* regulation in PDA, human cell lines were treated with the DNA methylase inhibitor 5-aza-2′-deoxycytidine and the HDAC inhibitor trichostatin A. Both inhibitors modestly increased the USP9X mRNA and protein levels in most cell lines, indicating that *USP9X* may be epigenetically silenced *in vivo* (Fig. 3d and Supplementary Fig. 15). Furthermore, although the promoter region of *USP9X* was not heavily methylated in tumour samples or PDA cells harbouring low protein expression (data not shown), treatment with 5-aza-2′-deoxycytidine did decrease colony formation of human PDA cells and this was partially reversed by concomitantly knocking down USP9X (Supplementary Fig. 16).

To confirm that $Kras^{G12D}$ cooperated with *Usp9x* loss to promote pancreatic cancer, a conditional $Usp9x^{fl}$ allele was generated (Supplementary Fig. 17a) and interbred with $Kras^{LSL\text{-}G12D}$; *Pdx1-cre* mice to evaluate the impact on mPanIN progression. The mosaic expression of Usp9x in pancreas from *Pdx1-cre;* $Usp9x^{fl/y}$ mice was confirmed by immunohistochemistry (Supplementary Fig. 17b). We found that all hemizygous male mice and heterozygous female mice carriers of the $Usp9x^{fl}$ allele in the background of $Kras^{LSL\text{-}G12D}$; *Pdx1-cre* rapidly developed advanced mPanIN and microinvasive neoplasms within 3 months of age (Fig. 3e, f and Supplementary Fig. 18). Immunohistochemical analysis of mPanINs from heterozygous female mice demonstrated absence of Usp9x expression in the pre-neoplastic and neoplastic cells (Supplementary Fig. 18), indicative of additional events such as X inactivation of the other locus in female mice[22,23]. mPanINs in $Kras^{LSL\text{-}G12D}$; *Pdx1-cre;* $Usp9x^{fl}$ mice expressed intranuclear Smad4, similar to $Kras^{LSL\text{-}G12D}$; *Pdx1-cre* mice (Supplementary Fig. 19a). Additionally, early passage pancreatic cell cultures

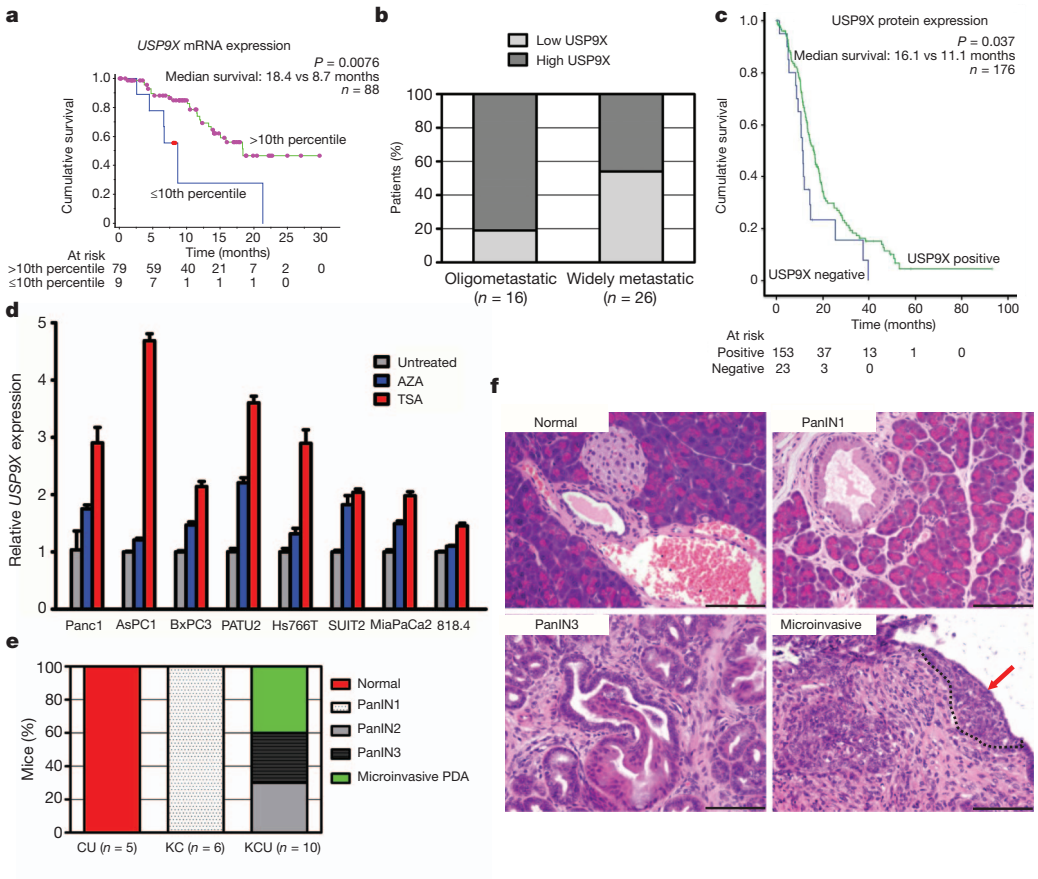

Figure 3 | *USP9X* loss promotes PDA. **a**–**c**, Decreased USP9X expression correlates with shortened survival in an Australian post-surgical cohort (**a**) (8.7 versus 18.4 months, $P = 0.0076$; log-rank test), increased metastatic burden in an American autopsy series (**b**) (54% versus 19%, $P = 0.0212$; Fisher's exact test), and diminished survival in a German post-surgical cohort (**c**) (11.1 versus 16.1 months, $P = 0.037$; log-rank test). **d**, Trichostatin A (TSA, red) and 5-aza-2′-deoxycytidine (AZA, blue) modestly increase *USP9X* mRNA expression in a panel of eight human PDA cell lines. The mean and s.e.m. of one representative experiment performed in triplicate are shown. **e**, *Usp9x* deletion promotes mPanIN progression in $Kras^{LSL\text{-}G12D}$; *Pdx1-cre;* $Usp9x^{fl/+}$ and $Kras^{LSL\text{-}G12D}$; *Pdx1-cre;* $Usp9x^{fl/y}$ (KCU) mice ($P < 0.0001$; Fisher's exact test). **f**, Representative normal pancreas (*Pdx1-cre;* $Usp9x^{fl/y}$; CU), mPanIN1 ($Kras^{LSL\text{-}G12D}$; *Pdx1-cre*; KC), mPanIN3 ($Kras^{LSL\text{-}G12D}$; *Pdx1-cre;* $Usp9x^{fl/+}$ and $Kras^{LSL\text{-}G12D}$; *Pdx1-cre;* $Usp9x^{fl/y}$; KCU) and microinvasive mPDA (KCU, arrow, circled). Scale bar: 100 μm.

prepared from these mice confirmed the absence of the Usp9x protein and altered regulation of Itch (Supplementary Fig. 19b). Although some mice died of local or metastatic pancreatic cancer, aggressive oral papillomas often required the culling of young mice and demonstrated that $Kras^{G12D}$ and *Usp9x* loss also cooperated to transform keratinocytes (Supplementary Fig. 19c).

Although a recent report implicated *USP9X* as a pro-survival gene by stabilizing MCL1 (ref. 9), potential inhibitors of USP9X should be developed with caution as we find that *Usp9x* has tissue-specific effects including a tumour suppressor role in oncogenic *Kras*-initiated pancreatic carcinoma. *USP9X* is probably epigenetically silenced in a subset of PDA, thus explaining why previous DNA sequencing efforts have failed to identify this as a participant in carcinogenesis, and indicating that clinically available epigenome modulators may be beneficial agents in such patients. ITCH is a likely mediator of pancreatic tumour suppression by USP9X, and continued investigation of the USP9X–ITCH pathway is warranted. More generally, the identification of *Usp9x* through the use of transposon mutagenesis reaffirms the utility of *in vivo* mouse cancer screens to complement the direct investigation of human cancer.

METHODS SUMMARY

$Kras^{LSL\text{-}G12D}$ (ref. 24), *Pdx1-cre* (ref. 8), *T2/Onc* (ref. 6), *CAGGS-SB10* (ref. 6) and *Rosa26-LSL-SB13* strains were interbred to generate $Kras^{LSL\text{-}G12D}$; *Pdx1-cre*, $Kras^{LSL\text{-}G12D}$; *Pdx1-cre; T2/Onc; CAGGS-SB10* and $Kras^{LSL\text{-}G12D}$; *Pdx-1-cre*; *T2/Onc*; *Rosa26-LSL-SB13* compound mutant mice. Non-quadruple mutant mice represented the comparison cohorts. $Kras^{LSL\text{-}G12D}$ and *Pdx1-cre* mice were interbred with $Usp9x^{fl}$ mice to generate the $Kras^{LSL\text{-}G12D}$; *Pdx1-cre;* $Usp9x^{fl/+}$ and $Kras^{LSL\text{-}G12D}$; *Pdx1-cre;* $Usp9x^{fl/y}$ compound mutant mice, as well as the two control cohorts *Pdx1-cre;* $Usp9x^{fl/y}$ and $Kras^{LSL\text{-}G12D}$; *Pdx1-cre. Usp9x*^{fl} mice were generated by Ozgene Pty. Ltd. Mice were maintained in compliance with the UK home office regulations. Splinkerette PCRs were performed as described previously[25,26]. Reads from sequenced tumours were mapped to the mouse genome assembly NCBI m37 and merged together to identify SB insertion sites, as previously described[25]. Redundant sequences, as well as insertions in the *En2* gene and in the *T2/Onc* donor concatemer resident chromosome (chromosome 1), were removed. Mouse survival curves and cell culture experiments were analysed with the GraphPad prism program. The IHC histoscoring from the TMA samples and Kaplan–Meier survival curves were analysed with SPSS18, and the Spearman-Rho correlation coefficient (two-sided) between USP9X and ITCH was calculated. The IHC USP9X histoscore and analysis was conducted using Fisher's exact test on post-mortem samples.

Full Methods and any associated references are available in the online version of the paper at www.nature.com/nature.

Received 30 May 2011; accepted 5 April 2012.
Published online 29 April 2012.

1. Almoguera, C. *et al.* Most human carcinomas of the exocrine pancreas contain mutant c-K-ras genes. *Cell* **53,** 549–554 (1988).
2. Caldas, C. *et al.* Frequent somatic mutations and homozygous deletions of the p16 (*MTS1*) gene in pancreatic adenocarcinoma. *Nature Genet.* **8,** 27–32 (1994).
3. Redston, M. S. *et al.* p53 mutations in pancreatic carcinoma and evidence of common involvement of homocopolymer tracts in DNA microdeletions. *Cancer Res.* **54,** 3025–3033 (1994).

4. Hahn, S. A. *et al.* DPC4, a candidate tumor suppressor gene at human chromosome 18q21.1. *Science* **271,** 350–353 (1996).
5. Jones, S. *et al.* Core signaling pathways in human pancreatic cancers revealed by global genomic analyses. *Science* **321,** 1801–1806 (2008).
6. Collier, L. S., Carlson, C. M., Ravimohan, S., Dupuy, A. J. & Largaespada, D. A. Cancer gene discovery in solid tumours using transposon-based somatic mutagenesis in the mouse. *Nature* **436,** 272–276 (2005).
7. Dupuy, A. J., Akagi, K., Largaespada, D. A., Copeland, N. G. & Jenkins, N. A. Mammalian mutagenesis using a highly mobile somatic *Sleeping Beauty* transposon system. *Nature* **436,** 221–226 (2005).
8. Hingorani, S. R. *et al.* Preinvasive and invasive ductal pancreatic cancer and its early detection in the mouse. *Cancer Cell* **4,** 437–450 (2003).
9. Schwickart, M. *et al.* Deubiquitinase USP9X stabilizes MCL1 and promotes tumour cell survival. *Nature* **463,** 103–107 (2010).
10. Keng, V. W. *et al.* A conditional transposon-based insertional mutagenesis screen for genes associated with mouse hepatocellular carcinoma. *Nature Biotechnol.* **27,** 264–274 (2009).
11. Starr, T. K. *et al.* A transposon-based genetic screen in mice identifies genes altered in colorectal cancer. *Science* **323,** 1747–1750 (2009).
12. Collier, L. S. *et al.* Whole-body sleeping beauty mutagenesis can cause penetrant leukemia/lymphoma and rare high-grade glioma without associated embryonic lethality. *Cancer Res.* **69,** 8429–8437 (2009).
13. Avizienyte, E. *et al.* LKB1 somatic mutations in sporadic tumors. *Am. J. Pathol.* **154,** 677–681 (1999).
14. Varela, I. *et al.* Exome sequencing identifies frequent mutation of the SWI/SNF complex gene *PBRM1* in renal carcinoma. *Nature* **469,** 539–542 (2011).
15. Su, G. H. *et al. ACVR1B* (*ALK4*, activin receptor type 1B) gene mutations in pancreatic carcinoma. *Proc. Natl Acad. Sci. USA* **98,** 3254–3257 (2001).
16. Li, M. *et al.* Deubiquitination of p53 by HAUSP is an important pathway for p53 stabilization. *Nature* **416,** 648–653 (2002).
17. Dupont, S. *et al.* FAM/USP9x, a deubiquitinating enzyme essential for TGFβ signaling, controls Smad4 monoubiquitination. *Cell* **136,** 123–135 (2009).
18. Nagai, H. *et al.* Ubiquitin-like sequence in ASK1 plays critical roles in the recognition and stabilization by USP9X and oxidative stress-induced cell death. *Mol. Cell* **36,** 805–818 (2009).
19. Sun, H. *et al.* Bcr-Abl ubiquitination and Usp9x inhibition block kinase signaling and promote CML cell apoptosis. *Blood* **117,** 3151–3162 (2011).
20. Mouchantaf, R. *et al.* The ubiquitin ligase itch is auto-ubiquitylated *in vivo* and *in vitro* but is protected from degradation by interacting with the deubiquitylating enzyme FAM/USP9X. *J. Biol. Chem.* **281,** 38738–38747 (2006).
21. Bernassola, F., Karin, M., Ciechanover, A. & Melino, G. The HECT family of E3 ubiquitin ligases: multiple players in cancer development. *Cancer Cell* **14,** 10–21 (2008).
22. Wang, X., Soloway, P. D. & Clark, A. G. Paternally biased X inactivation in mouse neonatal brain. *Genome Biol.* **11,** R79 (2010).
23. Yang, F., Babak, T., Shendure, J. & Disteche, C. M. Global survey of escape from X inactivation by RNA-sequencing in mouse. *Genome Res.* **20,** 614–622 (2010).
24. Jackson, E. L. *et al.* Analysis of lung tumor initiation and progression using conditional expression of oncogenic K-ras. *Genes Dev.* **15,** 3243–3248 (2001).
25. March, H. N. *et al.* Insertional mutagenesis identifies multiple networks of cooperating genes driving intestinal tumorigenesis. *Nature Genet.* **43,** 1202–1209 (2011).
26. Uren, A. G. *et al.* A high-throughput splinkerette-PCR method for the isolation and sequencing of retroviral insertion sites. *Nature Protocols* **4,** 789–798 (2009).

Supplementary Information is linked to the online version of the paper at www.nature.com/nature.

Acknowledgements We thank P. Labosky for assistance in generating the *Rosa26-LSL-SB13* mouse; B. Bhagavan for pathology consultation; M. Tsao for providing the HPDE cell line; and N. Copeland and K. Mann for sharing pre-published information. We thank A. Gopinathan, H. Tiriac, D. Engle, D. Chan, F. Connor, S. Derkits and other members of the Tuveson laboratory for assistance and advice, and the animal care staff and histology core at CRI, and The University of Minnesota's Mouse Genetics Laboratory. This research was supported by the University of Cambridge and Cancer Research UK, The Li Ka Shing Foundation and Hutchison Whampoa Limited, the NIHR Cambridge Biomedical Research Centre, and the NIH (2P50CA101955 SPORE grant to D.A.T., D.A.L. and C.A.I.-D.; grants CA62924, CA128920 and CA106610 to C.A.I.-D.; P50CA62924 SPORE grant to R.H.H. and C.A.I.-D.; and CA122183 to L.S.C.). D.J.A. is supported by Cancer Research UK and the Wellcome Trust. L.v.d.W. is supported by the Kay Kendall Leukemia Fund. C.P. is supported by Wilhelm Sander Stiftung (2009.039.1) and Deutsche Forschungsgemeinschaft (PI 341/5-1). A.V.B., D.K.C., S.M.G. and the APGI investigators are funded by the National Health and Medical research Council of Australia (NHMRC); Queensland Government; Cancer Council NSW; Australian Cancer Research Foundation; Cancer Institute NSW; The Avner Nahmani Pancreatic Cancer Research Foundation; and the R.T. Hall Trust. Additional support was obtained from Fundación Ibercaja (P.A.P.-M.).

Author Contributions P.A.P.-M. performed the majority of all experiments, designed experiments, analysed data, and wrote the manuscript. L.v.d.W. and J.A.B. performed *in vitro* experiments. S.S. and S.A.W. generated the conditional Usp9x mouse. L.S.C. provided the *CAGGS-SB10* and *T2/Onc* mice. A.G.R., A.L.S., K.A.T.S., J.J.t.H., J.d.R. and L.F.A.W. conducted the CIS data analysis. G.K., R.G., D.A., P.R., T.K. and C.P. generated data from resected pancreatic tumours. Allen Li, R.H.H., R.M., S.K., J.Y., Ang Li, M.G. and C.A.I.-D. analysed human samples from autopsy series, and analysed mouse pathology and methylation studies. C.H., D.L.S. and R.K. sequenced PDA human samples from autopsy series. A.P.K. provided statistical analyses for the human PDA data sets. APGI, D.K.C., S.M.G. and A.V.B. generated and analysed data from ICGC/APGI (International Cancer Genome Consortium/Australian Pancreatic Cancer Genome Initiative). D.A.L. provided the *CAGGS-SB10* and *T2/Onc* mice, and analysed data. D.J.A. and D.A.T. designed the study, analysed the data, and wrote the manuscript. All authors commented upon and edited the final manuscript.

Author Information The GEO accession number for the ICGC/APGI gene expression data is GSE36924. Reprints and permissions information is available at www.nature.com/reprints. The authors declare no competing financial interests. Readers are welcome to comment on the online version of this article at www.nature.com/nature. Correspondence and requests for materials should be addressed to D.J.A. (da1@sanger.ac.uk) or D.A.T. (david.tuveson@cancer.org.uk).

Australian Pancreatic Cancer Genome Initiative

Garvan Institute of Medical Research Andrew V. Biankin[1], Amber L. Johns[1], Amanda Mawson[1], David K. Chang[1], Mary-Anne L. Brancato[1], Sarah J. Rowe[1], Skye L. Simpson[1], Mona Martyn-Smith[1], Lorraine A. Chantrill[1], Venessa T. Chin[1], Angela Chou[1], Mark J. Cowley[1], Jeremy L. Humphris[1], Marc D. Jones[1], R. Scott Mead[1], Adnan M. Nagrial[1], Marina Pajic[1], Jessica Pettit[1], Mark Pinese[1], Ilse Rooman[1], Jianmin Wu[1], Roger J. Daly[1], Elizabeth A. Musgrove[1], Robert L. Sutherland[1]; **Queensland Center for Medical Genomics, Institute for Molecular Bioscience** Sean M. Grimmond[2], Nicola Waddell[2], Karin S. Kassahn[2], David K. Miller[2], Peter J. Wilson[2], Ann-Marie Patch[2], Sarah Song[2], Ivon Harliwong[2], Senel Idrisoglu[2], Craig Nourse[2], Ehsan Nourbakhsh[2], Suzanne Manning[2], Shivangi Wani[2], Milena Gongora[2], Matthew Anderson[2], Oliver Holmes[2], Conrad Leonard[2], Darrin Taylor[2], Scott Wood[2], Christina Xu[2], Katia Nones[2], J. Lynn Fink[2], Angelika Christ[2], Tim Bruxner[2], Nicole Cloonan[2], Felicity Newell[2], John V. Pearson[2]; **Royal North Shore Hospital** Jaswinder S. Samra[3], Anthony J. Gill[3], Nick Pavlakis[3], Alex Guminski[3], Christopher Toon[3]; **Bankstown Hospital** Andrew V. Blankin[4], Ray Asghari[4], Neil D. Merrett[4], David K. Chang[4], Darren A. Pavey[4], Amithabad Das[4]; **Liverpool Hospital** Peter H. Cosman[5], Kasim Ismail[5], Chelsie O'Connor[5]; **Westmead Hospital** Vincent W. Lam[6], Duncan McLeod[6], Henry C. Pleass[6], Virginia James[6]; **Royal Prince Alfred Hospital** James G. Kench[7], Caroline L. Cooper[7], David Joseph[7], Charbel Sandroussi[7], Michael Crawford[7]; **Fremantle Hospital** Michael Texler[8], Cindy Forrest[8], Andrew Laycock[8], Krishna P. Epari[8], Mo Ballal[8], David R. Fletcher[8], Sanjay Mukhedkar[8]; **Sir Charles Gairdner Hospital** Nigel A. Spry[9], Bastiaan DeBoer[9], Ming Chai[9], Kynan Feeney[9]; **St John of God Healthcare** Nikolajs Zeps[10], Maria Beilin[10]; **Royal Adelaide Hospital** Nam Q. Nguyen[11], Andrew R. Ruszkiewicz[11], Chris Worthley[11], Chuan P. Tan[11], Tamara Debrencini[11]; **Flinders Medical Center** John Chen[12], Mark E. Brooke-Smith[12], Virginia Papangelis[12]; **Greenslopes Private Hospital** Henry Tang[13], Andrew P. Barbour[13]; **Envoi Pathology** Andrew D. Clouston[14], Patrick Martin[14]; **Princess Alexanda Hospital** Thomas J. O'Rourke[15], Amy Chiang[15], Jonathan W. Fawcett[15], Kellee Slater[15], Shinn Yeung[15], Michael Hatzifotis[15], Peter Hodgkinson[15]; **Austin Hospital** Christopher Christophi[16], Mehrdad Nikfarjam[16], Victorian Cancer Biobank[17]; **Johns Hopkins Medical Institutes** James R. Eshleman[18], Ralph H. Hruban[18], Anirban Maitra[18], Christine A. Iacobuzio-Donahue[18], Richard D. Schulick[18], Christopher L. Wolfgang[18], Richard A. Morgan[18]; **ARC-NET Center for Applied Research on Cancer** Rita T. Lawlor[19], Stefania Beghelli[19], Vincenzo Corbo[19], Maria Scardoni[19], Claudio Bassi[19]; **University of California** Margaret A. Tempero[20]

Australian Pancreatic Cancer Genome Initiative

[1]The Kinghorn Cancer Centre, Garvan Institute of Medical Research, 372 Victoria Street, Darlinghurst, Sydney, New South Wales 2010, Australia. [2]Queensland Center for Medical Genomics, Institute for Molecular Bioscience, University of Queensland, St Lucia, Queensland 4072, Australia. [3]Royal North Shore Hospital, Westbourne Street, Saint Leonards, New South Wales 2065, Australia. [4]Bankstown Hospital, Eldridge Road, Bankstown, New South Wales 2200, Australia. [5]Liverpool Hospital, Elizabeth Street, Liverpool, New South Wales 2170, Australia. [6]Westmead Hospital, Corner of Hawkesbury and Darcy Roads, Westmead, New South Wales 2145, Australia. [7]Royal Prince Alfred Hospital, Missenden Road, Camperdown, New South Wales 2050, Australia. [8]Fremantle Hospital, Alma Street, Fremantle, Western Australia 6959, Australia. [9]Sir Charles Gardiner Hospital, Hospital Avenue, Nedlands, Western Australia 6009, Australia. [10]St John of God Healthcare, 12 Salvado Road, Subiaco, Western Australia 6008, Australia. [11]Royal Adelaide Hospital, North Terrace, Adelaide, South Australia 5000, Australia. [12]Flinders Medical Center, Flinders Drive, Bedford Park, South Australia 5042, Australia. [13]Greenslopes Private Hospital, Newdegate Street, Greenslopes, Queensland 4120, Australia. [14]Envoi Pathology, 1/49 Butterfield Street, Herston, Queensland 4006, Australia. [15]Princess Alexandria Hospital, Corner of Cornwall Street and Ipswich Road, Woolloongabba, Queensland 4102, Australia. [16]Austin Hospital, 145 Studley Road, Heidelberg, Victoria 3084, Australia. [17]Victorian Cancer Biobank, 1 Rathdowne Street, Carlton, Victoria 3053, Australia. [18]Johns Hopkins Medical Institutes, 600 North Wolfe Street, Baltimore, Maryland 21287, USA. [19]ARC-NET Center for Applied Research on Cancer, University of Verona, Via dell'Artigliere 19, 37129 Verona, Province of Verona, Italy. [20]University of California, San Francisco, 500 Parnassus Avenue, San Francisco, California 94122, USA.

METHODS

Mouse strains. *Kras*$^{LSL\text{-}G12D}$ (ref. 24), *Pdx1-cre* (ref. 8), *T2/Onc* (ref. 6), *CAGGS-SB10* (ref. 6) and *Rosa26-LSL-SB13* strains were interbred to generate *Kras*$^{LSL\text{-}G12D}$; *Pdx1-cre*; *T2/Onc*; *CAGGS-SB10* (KCTSB10) and *Kras*$^{LSL\text{-}G12D}$; *Pdx-1-cre*; *T2/Onc*; *Rosa26-LSL-SB13* (KCTSB13) compound mutant mice. Non-quadruple mutant mice represented the comparison cohorts. Genomic DNA from tumours developed in KCTSB10 and KCTSB13 mice was obtained using the Puregene Core Kit A (Qiagen) and splinkerette PCRs were performed as described previously[25,26]. For the KCU cohort, *Kras*$^{LSL\text{-}G12D}$ and *Pdx1-cre* mice were interbred with *Usp9x*^{fl} mice to generate the *Kras*$^{LSL\text{-}G12D}$; *Pdx1-cre*; *Usp9x*$^{fl/+}$ and *Kras*$^{LSL\text{-}G12D}$; *Pdx1-cre; Usp9x*$^{fl/y}$ (KCU) compound mutant mice, as well as the two control cohorts *Pdx1-cre; Usp9x*$^{fl/y}$ (CU) and *Kras*$^{LSL\text{-}G12D}$; *Pdx1-cre* (KC).

Generation of *Rosa26-LSL-SB13* knock-in mice. TL1 ES cells[27] were electroporated with linearized pRosa26-LSL-SA-SB13-BGHpolyA targeting construct and correctly targeted puromycin-resistant clones were identified by Southern blot. Two positives clones exhibiting a normal karyotype were used to generate chimaeric mice by microinjection into C57BL/6 blastocysts. Germline transmission of the targeted allele was confirmed by Southern blot analysis of tail DNA from the agouti offspring.

***T2/Onc* excision PCR.** Genomic DNAs were obtained from *Pdx1-cre; T2/Onc; Rosa26-LSL-SB13* and *T2/Onc; Rosa26-LSL-SB13* mice and primers used to assess the excision of the *T2/Onc* concatemer in the *Pdx1-cre; T2/Onc; Rosa26-LSL-SB13* mice were 5′-TGTGCTGCAAGGCGATTA-3′ and 5′-ACCATGATTACGCC AAGC-3′.

CIS analysis. For the statistical analysis, redundant sequences, as well as insertions in the *En2* gene and in the *T2/Onc* donor concatemer resident chromosome (chromosome 1), were removed and 90,007 non-redundant insertion sites (Supplementary Table 3) were used to identify CISs using a Gaussian kernel convolution framework (GKC)[28]. Reads from sequenced tumours were mapped to the mouse genome assembly NCBI m37 and merged together to identify SB insertion sites, as previously described[25]. An enhanced version of the framework was developed for SB screens to account for the local density of TA sites within the genome[25]. For example, a genomic region containing a large number of insertion sites but a low density of TA sites is considered to be significant and thereby identified as a candidate CIS. Conversely, a region with a large number of insertion sites but also containing a high density of TA sites is determined to be less significant, as the transposons have more 'target' sites into which they can integrate. Multiple kernel scales were used in the GKC framework (widths of 15K, 30K, 50K, 75K, 120K and 240K nucleotides). CISs predicted across multiple scales and overlapping in their genomic locations were clustered together, such that the CIS with the smallest genomic 'footprint' was reported as the representative CIS. For highly significant CISs with narrow spatial distributions of insertion sites, the 15K kernel is typically the scale on which CISs are identified. Additional statistical analysis of insertion sites was performed using a Monte Carlo framework[10]. CISs were compared to previously published data sets of human pancreatic cancer genetics[5,29,30].

Detection of *Usp9x-T2/Onc* fusion mRNA by RT–PCR in SB tumours. Total RNA was extracted from snap-frozen SB tumours using the RNeasy Mini kit (Qiagen), and total RNA (1 μg) was reverse transcribed into cDNA using the High Capacity RNA-to-cDNA kit (Applied Biosystems). RT–PCR was carried out with a nested PCR approach using primers of mouse *Usp9x* exon 1 and the Carp-β-actin splice acceptor sequence of the *T2/Onc* transposon cassette. cDNA was used as a template in a first round of PCR using specific primers corresponding to exon 1 of *Usp9x* (5′-GAGTCTGCGCTGCCGCTGCTG-3′) and Carp-β-actin splice acceptor sequence (5′-CATACCGGCTACGTTGCTAA-3′). The product of this reaction was used as a template in a second round of nested PCR using an internal primer in the *Usp9x* exon 1 (5′-GCTGCCGCTG CTGTTGCTGC-3′) and a second primer in the Carp-β-actin splice acceptor sequence (5′-ACGTTGCTAACAACCAGTGC-3′). PCR products were cloned into pCR 2.1-TOPO vector (Invitrogen) and positives clones sequenced.

Plasmids, shRNAs and transfections. pSuperRetro-PURO retroviral vector (Oligoengine) expressed a short hairpin against mouse and human *USP9X* (5′-GATGAGGAACCTGCATTTC-3′), mouse *Itch* (5′-GACCTGAGAAGACG TTTGT-3′)[31] and a scrambled sequence (5′-GCGCGCTTTGTAGGATTCG-3′). pBabe-zeo-Ecotropic receptor (ecoR) was obtained from Addgene (plasmid no. 10687). Myc-mItch cDNA was released from pCINeo-Myc-Itch (Addgene plasmid no. 11427), and was subcloned in the retroviral vector pBabe-neo (Addgene plasmid no. 1767). KCU1 and KCU2 cell lines were transfected with pEF-DEST51-mUsp9x(WT)-V5 and pEF-DEST51-mUsp9x(C1566S)-V5 plasmids[32,33]. The plasmid pEF/GW-51/LacZ (Invitrogen) was used as control. Transfections were done using Lipofectamine 2000 (Invitrogen). Twenty-four hours later, cells were selected with 5 μg ml^{-1} blasticidin (Invitrogen).

Cell culture. Tumour pancreatic cancer cell lines were established from *Kras*$^{LSL\text{-}G12D}$; *Pdx1-cre* (T4878 and T9394), *Kras*$^{LSL\text{-}G12D}$; *P48-cre* (TB1572) and *Kras*$^{LSL\text{-}G12D}$; *Pdx-1-Cre; Usp9x*^{fl} (KCU1 and KCU2) mice as described previously[34]. Cells were subsequently cultured in DMEM (Invitrogen), supplemented with 10% FCS (Hyclone). The normal human pancreatic ductal cell line HPDE was provided by M. Tsao and cultured as described previously[35,36]. The human pancreatic cancer cell lines AsPC1 (CRL-1682) and BxPC3 (CRL-1687) were acquired from ATCC and cultured according to instructions. The other cell lines were obtained from Clare Hall Laboratories (CRUK). The human cell lines Panc1, MiaPaCa2, 818.4, Hs766T, PATU2, SUIT2, FA6 and MDA-Panc3 (PDA); CaCO2 and SW1116 (colorectal cancer); SKBR3 (breast cancer) and A549 (lung cancer) were cultured in DMEM supplemented with 10% FCS. The human cell lines U937 (histiocytic lymphoma), RAMOS (Burkitt's lymphoma), NCI-H2179 (lung cancer) and ZR75-1 (breast cancer) were cultured in RPMI (Invitrogen) supplemented with 10% FCS. Cells were treated with 1 μM trichostatin A (Sigma) for 24 h or with 5 μM 5-aza-2′-deoxycytidine (Sigma) for 96 h where indicated to obtain RNA and protein lysates to assess USP9X expression. For anchorage-independent growth assay, cells were treated with 5 μM 5-aza-2′-deoxycytidine (Sigma).

Retroviral infections. Phoenix cells were plated 24 h before transfection using the ProFection Mammalian Transfection System Calcium Phosphate (Promega). Target cells were infected with retroviruses produced in the Phoenix packaging cells (24 and 48 h after transfection) in the presence of 8 μg ml^{-1} polybrene (Sigma) and were selected with 2 μg ml^{-1} puromycin (Sigma) or 1 mg ml^{-1} G418 (Clontech). Experiments were performed using at least two independent cell line infected pools. Human PDA cells lines Panc1, SUIT2 and PATU2 infected with retroviral vectors expressed the ecotropic receptor (ecoR).

Transformation, anoikis and EMT assays. Cell lines (1.5×10^4 cells) were plated in triplicate in 12-well plates and counted as indicated using a Z2 Coulter (Beckman). Cells were fed every other day. Anchorage-independent growth was assessed by colony formation in soft agar. Briefly, 15,000 cells were plated in duplicate in DMEM with 15% serum and 0.34% low-melting-point agarose (LMP, BioGene) onto 6-cm dishes coated with 0.5% LMP. Cells were fed twice a week and grown for 2 weeks. Colonies were counted in nine different ×20 fields. For the anoikis assay, 10^5 cells per 0.5 ml were plated in 24-well ultra-low cluster plates (Costar) to allow them to grow in suspension for 4 days. Cells were collected, washed with cold PBS and protein lysates were obtained. Cell line T4878 was cultured in matrigel as previously described[37], plating 1,000 cells per well. Cells were fed every 2 days and grown for 4 days. Epithelial-to-mesenchymal transition (EMT) was determined by plating 10^5 cells per 6-well plates for 24 h to allow attachment, followed by treatment with human TGF-β1 (5 ng ml^{-1}) (RD Systems) for 24 h. p21 induction was assessed after treatment with human TGF-β1 (5 ng ml^{-1}) (RD Systems) for 2 h.

Real-time PCR. Total RNA from human PDA cell lines was extracted using the RNeasy Mini Kit (Qiagen), and total RNA (1 μg) was reverse transcribed into cDNA using the High Capacity RNA-to-cDNA kit (Applied Biosystems). Human *USP9X* expression was analysed by quantitative PCR (qPCR) using TaqMan gene expression assays Hs00245009_m1 (Applied Biosystems) on a 7900HT Real-Time PCR system (Applied Biosystems). Gene expression was normalized to human *ACTB* expression, assessed with the gene expression assays Hs99999903_m1 (Applied Biosystems), and shown relative to control samples.

Western blot analysis. Cells were washed three times in cold PBS and lysed with boiling lysis buffer (1% SDS, 10 mM, pH 7.5 Tris, 50 mM NaF, 1 mM Na_3VO_4). Lysates were boiled for 5 min, passed through a 26 gauge needle to shear genomic DNA and centrifuged for 10 min at 14,000 r.p.m. Equivalent amounts of protein were resolved in 4–12% gradient SDS–PAGE gels (Invitrogen), transferred to Immobilon–P transfer membranes (Millipore), and incubated with the corresponding antibodies including anti-Ask1 (NB110-55482, Novus Biologicals), anti-Mcl1 (5453, Cell Signaling), anti-Usp9x (A301-351A, Bethyl), anti-CC3 (9664, Cell Signaling), anti-Itch (611198, BD), anti-p21 (sc-6246, Santa Cruz), anti-Smad4 (sc-7966, Santa Cruz), anti-Myc tag (2276, Cell Signaling), anti V5 tag (R960-25, Invitrogen), anti-c-Flip (ALX-804-127, Enzo Life Sciences), anti-c-Jun (9165, Cell Signaling), anti-p63 (Ab110038, Abcam), anti-α-Tubulin (T6074, Sigma) and anti-Actin (sc-1616, Santa Cruz Biotechnology). Reactive bands were visualized with ECL plus reagent (Amersham). Relative expression was quantified with Image Quant TL software (GE Healthcare).

Immunohistochemistry. Formalin-fixed paraffin-embedded (FFPE) mouse tissues were cut into 3-μm tissue sections, and antigen retrieval was performed in 10 mM, pH 6.0 citric acid (for Usp9x and E-cadherin) or 10 mM, pH 8.0 EDTA (for Smad4). Endogenous peroxidases were quenched in 3% H_2O_2/PBS for 20 min. Signal detection for immunohistochemistry was accomplished with biotinylated secondary antibodies (Vector Laboratories) using the Elite Vectastain ABC kit and peroxidase substrate DAB kit (Vector Laboratories). Primary antibodies used were anti-Usp9x, 1:200 (A301-351A, Bethyl); E-cadherin, 1:200 (610182, BD) and

anti-Smad4, 1:100 (sc-7966, Santa Cruz). Slides were counterstained with haematoxylin.

Clinical patient samples immunohistochemistry and analysis. Tissue microarrays ($n = 404$) were prepared from patient samples obtained after appropriate informed consent in Dresden (Institute of Pathology, University Hospital Dresden), Regensburg (Institute of Pathology, University Hospital Regensburg) and Jena (Institute of Pathology, University Hospital Jena). Informed consent was obtained for each patient, following review by the human ethics committee Ethikkommission an der Technischen Universität Dresden. The PDA tumour samples were collected from 1993 to 2009, and most of the patients (65%) did not undergo adjuvant chemotherapy. Those that did undergo adjuvant therapy (35%) were chiefly treated with 5FU or gemcitabine-based regimens, but in this subgroup there was no significant increase in patient survival. The median survival times of patients after surgery from each centre were indistinguishable. Immunohistochemistry was performed on 5 μm sections that were prepared using silanized slides (Menzel Gläser). Staining was performed with the Benchmark System (Ventana), using rabbit anti-USP9X antibody, 1:200 (A301-351A, Bethyl) and anti-ITCH, 1:200 (611198, BD); and the protocol UltraView HRP, with the CC1 modified protocol as pre-treatment. Slides were counterstained with haematoxylin. Staining intensities were scored as absent (0), weak (1), medium (2) and strong (3). For further analysis the staining intensities were grouped as negative (0) and positive (1–3). The Cox regression model assumption of proportional hazard was tested using a plot of the cumulative hazards function.

A second cohort of patient samples was obtained from the Gastrointestinal Cancer Rapid Medical Donation Program in the Department of Pathology at Johns Hopkins Hospital, USA. Use of all human tissue samples from resection specimens and autopsy participants was approved by Johns Hopkins Institutional Review Board, and obtained after informed consent. All samples were collected within 12 h post mortem and formalin fixed before paraffin embedding. Five-micrometre sections were cut from matched primary and metastasis samples onto glass slides. Slides were first incubated in Dako Target Retrieval Solution for antigen retrieval. Slides were then incubated with rabbit anti-USP9X antibody, 1:1,000 (ab26334, Abcam) or 1:200 (NBP1-48321, Novus Biologicals), and anti-SMAD4 as previously described[38]. Signal detection for immunohistochemistry was accomplished with Dako LSAB+System-HRP. Slides were counterstained with haematoxylin.

An additional cohort of pancreatic cancer resection samples was prospectively acquired through the Australian Pancreatic Cancer Network and the Australian Pancreatic Cancer Genome Initiative (http://www.pancreaticcancer.net.au/apgi). Consent was obtained for genomic sequencing through the Australian Pancreatic Cancer Genome Initiative (APGI) for each individual patient following approval from Human Research Ethics Committees (HREC) at participating sites (Sydney South West Area Health Service HREC Western Zone, 2006/054; Sydney Local Health Network HREC RPA Zone, X11-0220; and North Sydney Central Coast Health, Harbour HREC, 0612-251M). We extracted RNA from tumour samples using the Qiagen Allprep kit (Qiagen) in accordance with the manufacturer's instructions, assayed for quality on an Agilent Bioanalyzer 2100 (Agilent Technologies), and subsequently hybridized to Illumina Human HT-12 V4 microarrays. Raw idat files were processed using IlluminaGeneExpressionIdatReader (M. Cowley *et al.*, manuscript in preparation). After array quality control, these data were vs.t transformed, and then robust spline normalized, using the lumi R/Bioconductor package. For the ICGC/APGI cohort, we assumed a proportional hazard: that the probability of death is the same for those censored as for those remaining on study.

For the TMA and expression array cohorts, median survival was estimated using the Kaplan–Meier method and the difference was tested using the log-rank test. P values of less than 0.05 were considered statistically significant. For the TMA cohort, as few parameters were significant in univariate analysis, all were initially considered for Cox Proportional Hazard multivariate analysis in a backward elimination model, and assessed with the SPSS18 Software (IBM) with overall survival used as the primary endpoint. For the ICGC/APGI cohort, clinicopathological variables analysed with a P value of less than 0.25 on log-rank test were entered into Cox proportional hazard multivariate analysis and the model was resolved using backward elimination. Statistical analysis was performed using StatView 5.0 Software (Abacus Systems). Disease-specific survival was used as the primary endpoint.

27. Tompers, D. M. & Labosky, P. A. Electroporation of murine embryonic stem cells: a step-by-step guide. *Stem Cells* **22,** 243–249 (2004).
28. de Ridder, J., Uren, A., Kool, J., Reinders, M. & Wessels, L. Detecting statistically significant common insertion sites in retroviral insertional mutagenesis screens. *PLOS Comput. Biol.* **2,** e166 (2006).
29. Grützmann, R. *et al.* Gene expression profiling of microdissected pancreatic ductal carcinomas using high-density DNA microarrays. *Neoplasia* **6,** 611–622 (2004).
30. Pilarsky, C. *et al.* Activation of Wnt signalling in stroma from pancreatic cancer identified by gene expression profiling. *J. Cell. Mol. Med.* **12,** 2823–2835 (2008).
31. Oberdoerffer, P. *et al.* Efficiency of RNA interference in the mouse hematopoietic system varies between cell types and developmental stages. *Mol. Cell. Biol.* **25,** 3896–3905 (2005).
32. Nathan, J. A. *et al.* The ubiquitin E3 ligase MARCH7 is differentially regulated by the deubiquitylating enzymes USP7 and USP9X. *Traffic* **9,** 1130–1145 (2008).
33. Murray, R. Z., Jolly, L. A. & Wood, S. A. The FAM deubiquitylating enzyme localizes to multiple points of protein trafficking in epithelia, where it associates with E-cadherin and beta-catenin. *Mol. Biol. Cell* **15,** 1591–1599 (2004).
34. Olive, K. P. *et al.* Inhibition of Hedgehog signaling enhances delivery of chemotherapy in a mouse model of pancreatic cancer. *Science* **324,** 1457–1461 (2009).
35. Ouyang, H. *et al.* Immortal human pancreatic duct epithelial cell lines with near normal genotype and phenotype. *Am. J. Pathol.* **157,** 1623–1631 (2000).
36. Furukawa, T. *et al.* Long-term culture and immortalization of epithelial cells from normal adult human pancreatic ducts transfected by the E6E7 gene of human papilloma virus 16. *Am. J. Pathol.* **148,** 1763–1770 (1996).
37. Debnath, J., Muthuswamy, S. K. & Brugge, J. S. Morphogenesis and oncogenesis of MCF-10A mammary epithelial acini grown in three-dimensional basement membrane cultures. *Methods* **30,** 256–268 (2003).
38. Iacobuzio-Donahue, C. A. *et al.* DPC4 gene status of the primary carcinoma correlates with patterns of failure in patients with pancreatic cancer. *J. Clin. Oncol.* **27,** 1806–1813 (2009).